European Review for Medical and Pharmacological Sciences 2020; 24: 7240-7252

Whole-body magnetic resonance imaging is superior to skeletal scintigraphy for the detection of bone metastatic tumors: a meta-analysis

G. SUN[1], Y.-X. ZHANG[2], F. LIU[3], N. TU[4]

[1]Department of Radiology, Zaozhuang Hospital of Traditional Chinese Medicine, Zaozhuang, Shandong, China
[2]No. 2 Department of Orthopedics, Zaozhuang Hospital of Traditional Chinese Medicine, Zaozhuang, Shandong, China
[3]Zaozhuang Hospital of Traditional Chinese Medicine, Zaozhuang, Shandong, China
[4]Department of Magnetic Resonance, Zaozhuang Municipal Hospital, Zaozhuang, Shandong, China

Gang Sun and Yongxiang Zhang contribute equally to this work

Abstract. – OBJECTIVE: The meta-analysis aims to compare the diagnostic performance of whole-body magnetic resonance imaging (MRI) and skeletal scintigraphy (SS) for the detection of skeletal metastases.

MATERIALS AND METHODS: We searched Medline, Scopus, Embase and Cochrane library databases for identifying fifteen eligible studies with a total of 1939 participants, and the quality of these studies was assessed according to Quality Assessment of Diagnostic Accuracy Studies (QUADAS-2) guidelines. Sensitivities, specificities, diagnostic odds ratios (DOR), positive likelihood ratios (PLR), and negative likelihood ratios (NLR) were calculated. Summary receiver operating characteristic curves (sROC) were generated using bivariate models for whole-body MRI and skeletal scintigraphy.

RESULTS: Whole-body MRI had higher but comparable patient-based higher specificity compared to SS (99% vs. 95%). However, it had markedly higher sensitivity (94% vs. 80% respectively), DOR (966 vs. 82), and LPR (54.4 vs 17.1). LNR of whole-body MRI was <0.1 (0.06), while LNR of SS was >0.1 (0.22). The area under curves (AUC) for whole-body MRI and SS were 0.99 and 0.95 respectively.

CONCLUSIONS: We demonstrate that both whole-body MRI and SS have good diagnostic performance. However, MRI is superior for diagnostics of bone metastases, as it has higher sensitivity, higher diagnostic accuracy, and can be used for both confirmation and exclusion of metastatic bone disease.

Key Words:
Magnetic resonance imaging, Skeletal scintigraphy, Bone metastatic tumors, Meta-analysis.

Introduction

Any type of metastatic cancer that spreads via the bloodstream can infiltrate the bone marrow and give rise to bone metastases[1,2]. Certain types of cancers, such as prostate or breast cancer, are known for their ability to cause skeletal metastases, with a prevalence of up to 70%[3,4]. There is high variability in the metabolic activity of different types of bone metastases. It is therefore important to choose the suitable diagnostic method among a variety of radiological and nuclear medical imaging techniques for the detection of bone metastases in patients with certain types of cancers.

Skeletal scintigraphy (SS) with labeled phosphonates (^{99M}TC-phosphonates) is routinely used for the detection of local bone metabolism in an early phase of some types of cancers[5]. Therefore, SS is most effective in the visualization of metastases that are associated with reactive hypermetabolism of bone. This includes metastases of prostate and breast cancer, neuroendocrine tumors, and osteosarcomas[5-8]. However, SS is relatively insensitive for tumors that are not hypermetabolic and can lead to false-positive results in cases of post-treatment bone matrix regeneration (flare phenomenon)[9].

Magnetic resonance imaging (MRI) is quickly becoming a method of choice for detecting bone metastases due to its high soft-tissue contrast, high spatial resolution, and no requirements for intravenous contrast medium[10]. In the 2011 me-

Corresponding Author: Nan Tu, MD; e-mail: fhr15563002236@163.com

ta-analysis, Yang et al[11] showed that MRI had 91% sensitivity and 95% specificity, being superior to planar skeletal scintigraphy. These findings were further confirmed in subsequent studies involving, among others, breast, prostate, lung and renal cancers[13-23]. However, these studies have certain limitations, such as a lack of pathological verification of skeletal metastases, selection bias, and not taking into consideration an improved SS with the use of more advanced single-photon-emission computerized tomography/combined with CT (SPECT/SPECT-CT) apparatus[17,24,25].

The purpose of this meta-analysis is to compare the efficiency of whole-body MRI and skeletal scintigraphy in the detection and characterization of skeletal metastases.

Materials and Methods

Eligibility Criteria

The inclusion criteria were as follows: studies comparing the diagnostic performance of skeletal scintigraphy and whole-body MRI irrespective of study design employed; studies that report required statistics of the above-mentioned techniques or provide data to calculate these rates; full-text studies or published as conference abstracts were included while unpublished data, case reports, and studies with smaller sample size (fixed at 10 for the current review) were excluded.

Participants: patients with a primary malignant tumor in sites other than skeletal sites.

Index test: studies that used skeletal scintigraphy and whole-body MRI for the identification of bone metastasis.

Reference standards: studies where the diagnostic accuracy is compared with a definitive diagnosis of bone metastasis by histopathological or biopsy findings.

Type of Outcome Measure

Pooled sensitivity, specificity, positive likelihood ratio (PLR) and negative likelihood ratio (NLR) and diagnostic odds ratio (DOR)

Search Strategy

For this meta-analysis, we identified relevant studies by searching the following Medline, Scopus, Embase and Cochrane library databases. The following medical subject headings (MeSH terms) and free-text terms were used in PubMed in several combinations: "Validation Studies", "Bone Metastasis", "Skeletal Metastasis", "Bone Scintigraphy", "Skeletal Scintigraphy", "Magnetic Resonance Imaging", "Sensitivity", "Specificity", "Diagnosis", and "Diagnostic Accuracy Studies". Similar terms were also used in Cochrane library, Scopus, Embase for literature search of published studies. The time period was from inception to December 2019 without any language restrictions. Bibliographies of retrieved studies were searched, and eligible studies were included.

Study Selection

Two authors independently screened the title and abstract of the records identified during the literature search. The full-text article was retrieved for studies deemed relevant. The further full-text screening was again done by the two authors independently and those studies matching the inclusion criteria were finally included in our review. Disagreements between the two authors during this process were solved via consultation with a third investigator.

Data Extraction Process

Data extraction for the required characteristics from the included studies was done by the primary investigator. The data extracted were study design, setting, index test, reference standards (gold standard/comparator), comorbidities, the total number of participants, average age, inclusion, exclusion criteria, sensitivity, and specificity. The extracted data were transferred into STATA software.

Risk of Bias Assessment In Included Studies

The risk of bias was assessed by two authors independently using the Quality Assessment of Diagnostic Accuracy Studies-2 (QUADAS-2) tool. Domains used for assessing the risk of bias were the selection of patients, characteristics of index test and reference standard, timing, and flow of assessments. The risk of bias was finally interpreted as low, high or unclear.

Statistical Analysis

Meta-analysis was done with the selected studies using STATA 14.2 software (StataCorp, College Station, TX, USA). Bivariate meta-analysis was done to obtain the pooled estimates of the diagnostic accuracy estimates like sensitivity and specificity, PLR and NLR, and DOR for MRI and Skeletal Scintigraphy. Summary Receiver Operator Characteristic curves (sROC) was made. The summary estimate obtained in the sROC was the area under the curve (AUC) with 95% confidence

interval (CI). AUC value closer to 1 indicates the higher diagnostic performance of the imaging techniques.

Forest plot was used to graphically represent the study level and overall pooled diagnostic measures. Likelihood ratio (LR) scattergram was made to find the clinical significance of these imaging techniques. Fagan plot was constructed to demonstrate how much the result of MRI or Skeletal Scintigraphy changes the probability that a patient has a diagnosis of bone metastases.

Heterogeneity was evaluated via the following methods: graphical representation through bivariate box plot, Chi-square test for heterogeneity and I^2 statistics to quantify the inconsistency. Potential sources of heterogeneity were explored by meta-regression using potential predictive covariates like quality-related factors (under QUADAS). A funnel plot was used to graphically represent the publication bias and tested by Deek's test.

Results

Search Results

We have conducted a systematic search to find studies reporting the diagnostic performance of MRI and SS for the diagnosis of bone metastases. Totally, 2834 records found, out of which 1189 studies from Medline, 835 from Scopus, 598 from Embase, and 212 from the Cochrane library (Figure 1). After the removal of duplicates, the remaining 2178 studies were subjected to the title, abstract and keywords screening. At that stage, 1981 studies were eliminated, due to different outcomes (n=1480) and irrelevant diagnoses (n=501). Full text of 197 relevant studies was reviewed for eligibility criteria. Of them, 111 studies were eliminated due to different outcomes, 21 studies described different diseases, and 50 studies were excluded after the bibliography review. The remaining 15 potential studies

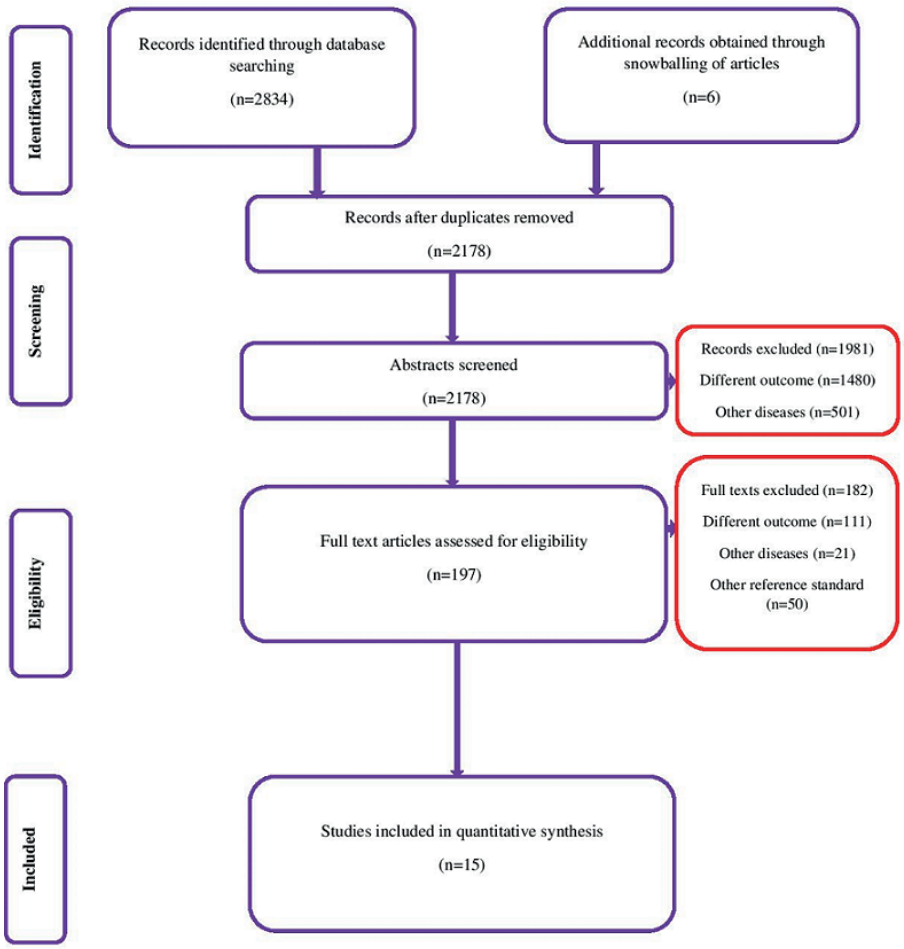

Figure 1. Search strategy.

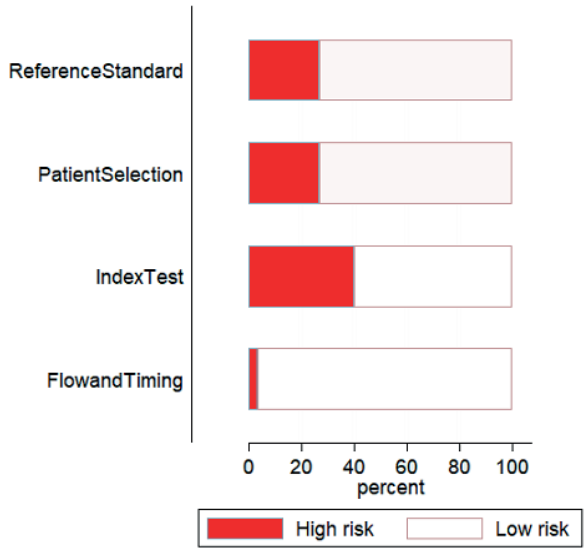

Figure 2. Quality assessment among the included studies using QUADAS-2 tool (n=15).

satisfied the eligibility criteria, with 1939 participants (Figure 1).

Characteristics of the Included Studies

Characteristics of the studies were described in Table I. Majority (12) of included studies are prospective studies[14,16,17,21,26-33], 2 studies were retrospective[34,35], and one study was a clinical trial[36]. The age of participants ranged from 2 to 82 years. In total, 1939 participants were found in the included studies with sample size varying from 22 to 1025, and the follow-up time ranging from 6 months to 2 years. All the included studies have documented histology or biopsy results as a reference standard. Majority of the studies (13) used 1.5T strength MRI[14,16,17,21,26-29,31-34,36]. The amount of ^{99M}TC ranged from 500 to 925 MBq (Table I).

The Methodological Quality of the Included Studies

Patient selection bias assessment demonstrated that almost 75% of the studies had a low risk of bias. Assessment of bias due to conduct and interpretation of the index test domain showed that 60% of the studies had a low risk of bias. 75% of the included studies had a low risk of bias for conduct and interpretation of reference standards, while only 5% of the studies demonstrated bias due to flow and timing of assessments (Figure 2).

Diagnostic Performance of MRI and SS

As summarized in Figure 3 and Table II, pooled sensitivity of MRI was 94% (95% CI: 87%-98%), pooled specificity was 98% (95% CI: 97%-99%) and DOR was 966 (95% CI: 264-3543). PLR was 54.4 (95% CI: 27.3-108.3) and NLR was

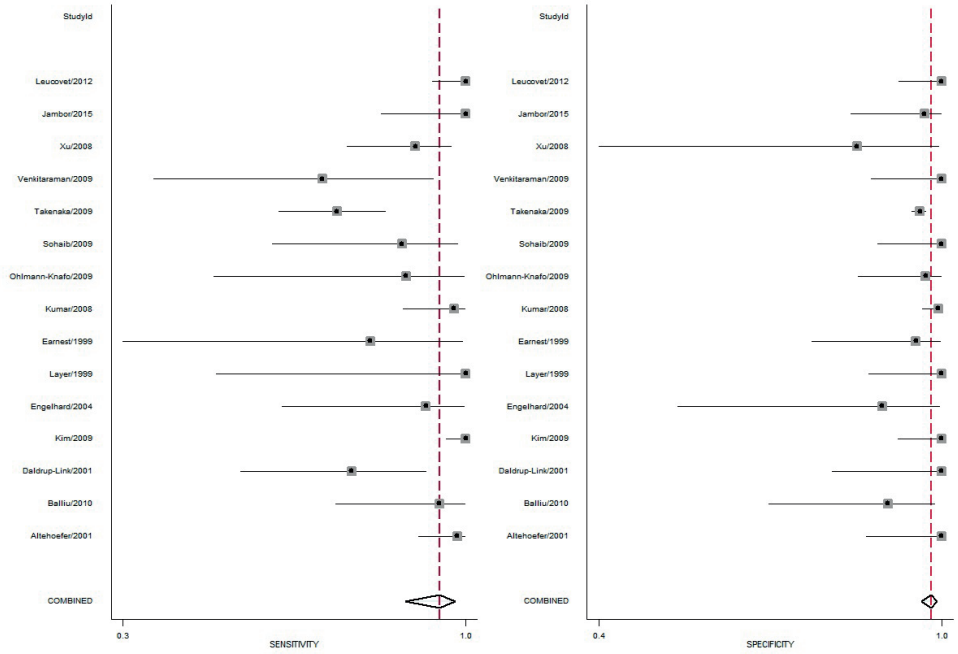

Figure 3. Forest plot showing pooled sensitivity and specificity for MRI.

Table I. Characteristics of the included studies (N=15).

Study No	First author and year	Country	Study design	Sample size	Follow-up time & Sequences	MRI Strength	Skeletal scintigraphy Amount of 99MTC & Delay time	Mean age (in years)
1	Daldrup-Link et al[26] 2001	Germany	Prospective	39	>10 months	1.5 T T1, T2, STIR	740 MBq 3-4h	2-19
2	Engelhard et al[21] 2004	Germany	Prospective	22	>12 months	1.5T T1, T2, STIR	550 MBq 2-3h	53-87
3	Sohaib et al[17] 2009	United Kingdom	Prospective	47	>12 months	1.5T T1, STIR	600 MBq 3h	29-79
4	Takenaka et al[27] 2009	Japan	Prospective	115	>12 months	1.5T T1, STIR	555 MBq 3h	72
5	Venkitaraman et al[28] 2009	United Kingdom	Prospective	39	>657 days	1.5T T1, STIR	640 MBq 3h	54-82
6	Balliu et al[29] 2010	Spain	Prospective	40	>12 months	1.5T T1, STIR	925 MBq 2 hours	62.1
7	Kim et al[30] 2009	Korea	Retrospective	134	2 years	3T T1, T2, STIR	750 MBq 3 hours	50
8	Lecouvet et al[16] 2012	Belgium	Prospective study	100	6 months	1.5T T1, STIR	Not specified	69
9	Altehoefer et al[35] 2001	Germany	Retrospective study	81	11 months	3T T1, T2, STIR	500-650 MBq 2-4h	Not specified
10	Earnest et al[31]1999	United States of America	Prospective	29	12 months	1.5T T1, T2, STIR	Not specified	67.2
11	Jambor et al[36] 2015	Finland	Clinical trial	53	15 months	1.5T T1, T2, STIR	670 MBq 3h	Not specified
12	Kumar et al[34] 2008	India	Retrospective	208	16 months	1.5T T1	2-4 hours	Not specified
13	Layer et al[32] 1999	Germany	Prospective	33	Not specified	1.5T T1	Not specified	Not specified
14	Ohlmann-Knafo et al[14] 2009	Germany	Prospective randomized controlled trial	45	Not specified	1.5T T1, T2, STIR	Not specified	Not specified
15	Xu et al33 2008	China	Prospective	45	2 months	1.5T T1, T2, STIR	2 hours	52.7

DOR: diagnostic odds ratio; LPR: positive likelihood ratios; LNR: negative likelihood ratio; AUC: area under sROC curve; 95% CI: 95% confidence interval.

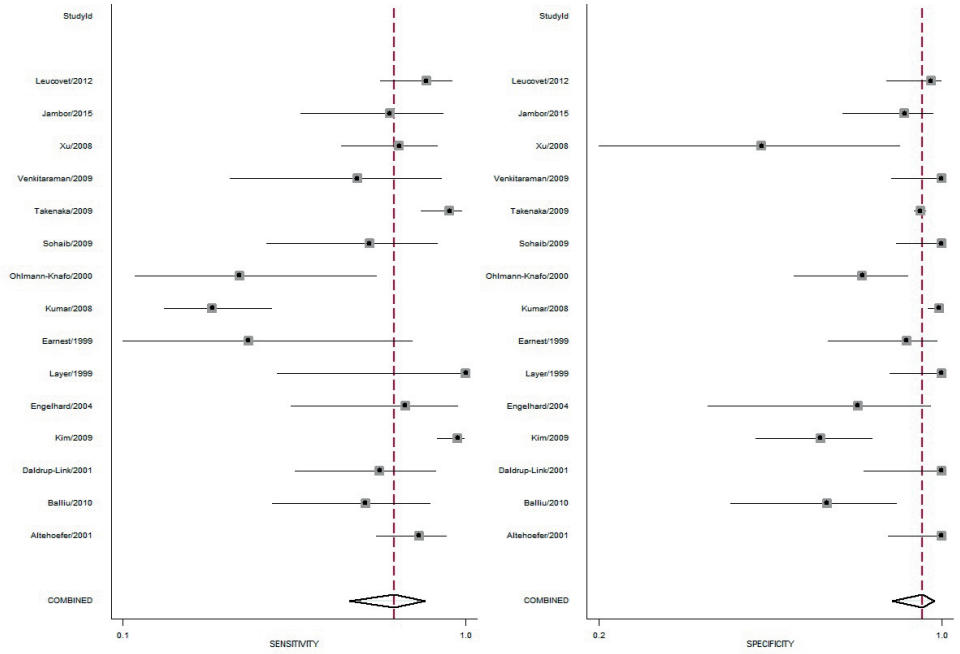

Figure 4. Forest plot showing pooled sensitivity and specificity for SS.

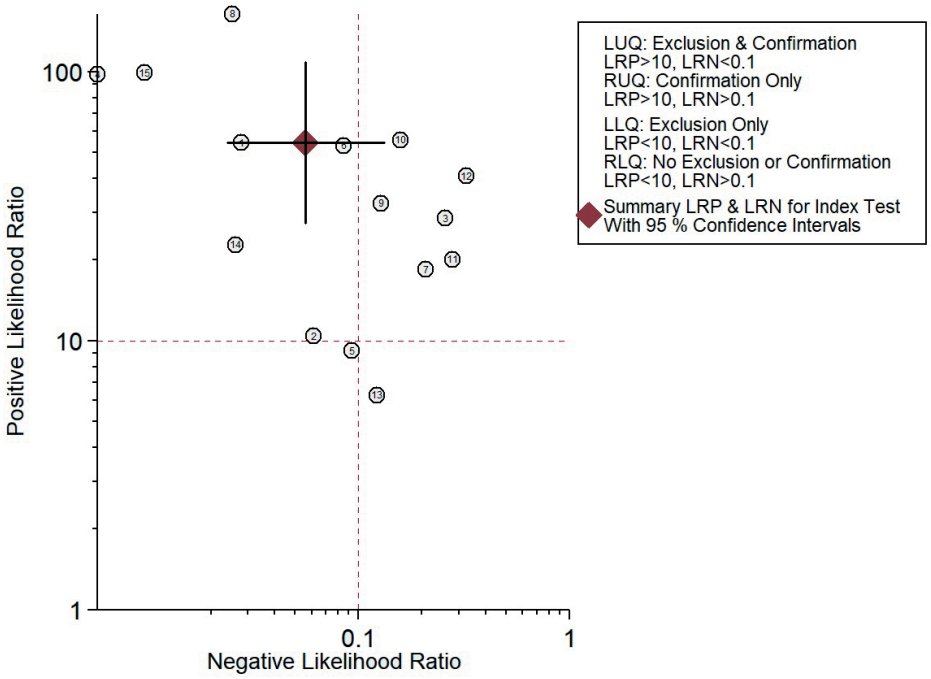

Figure 5. Likelihood scattergram for MRI.

Table II. Accuracy of whole-body MRI and SS.

	Sensitivity (95% CI)	Specificity (95% CI)	DOR (95% CI)	LPR (95% CI)	LNR (95% CI)	AUC (95% CI)
Whole-body MRI	94% (87%-98%)	99% (97%-99%)	966 (264-3543)	54.4 (27.3-108.3)	0.06 (0.02-0.13)	0.99(1.00-0.0)
Skeletal scintigraphy	80% (68%-89)	95% (88%-98)	82 (27-248)	17.1 (6.6-43.9)	0.21 (0.12-0.3)	0.95 (1.00-0.0)

DOR: diagnostic odds ratio; LPR: positive likelihood ratios; LNR: negative likelihood ratio; AUC: area under sROC curve; 95% CI: 95% confidence interval.

0.06 (0.02-0.13). The pooled sensitivity of skeletal scintigraphy was 80% (95% CI: 68%-89%), pooled specificity was 95% (95% CI: 88%-98%) and DOR was 82 (95% CI: 27-248). PLR was 17.1 (95% CI: 6.6-43.9) and NLR was 0.21 (0.12-0.35) (Table II, Figure 4).

An LR scattergram was then generated to assess the clinical performance of whole-body MRI and SS diagnostic methods (Figures 5 and 6). For whole-body MRI, six of the included studies were plotted in the left upper quadrant of the scattergram[14,16,21,26,27,29]. While 6 additional studies were plotted to the upper right quadrant[17,30,31,34-36], one study in the lower-left quadrant[28], and one study in the lower-right quadrant[32], summarized PLR and NLR was localized to the left upper quadrant (95% CI) (Figure 5). For the SS, 6 of the included studies were plotted to the upper-right quadrant of the LR[16,17,26,31,34], 6 to the lower-right quadrant[14,21,28,30,32,35], 2 studies to the upper-left quadrant[29,36], and one study to the lower left quadrant[27]. A summarized PLR and NLR were positioned in the right upper quadrant in the LR scattergram (Figure 6).

We then constructed an sROC to assess the tradeoff between sensitivity and specificity. The AUC was 0.99 (95% CI, 1.00 to 0.00) for the MRI (Table II, Figure 7), and 0.95 (CI 95%, 1.00 to 0.00) for the SS (Table II, Figure 8).

Figures 9 and 10 show Fagan's nomogram for LR, found *post*-test probabilities from various pre-test probabilities. Our results indicated that

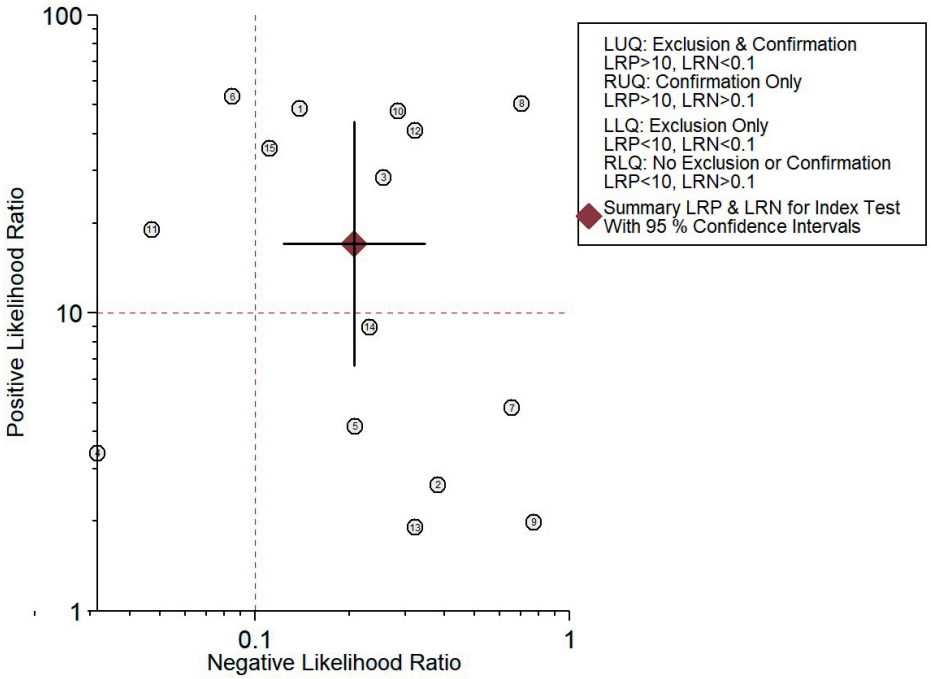

Figure 6. Likelihood scattergram for SS.

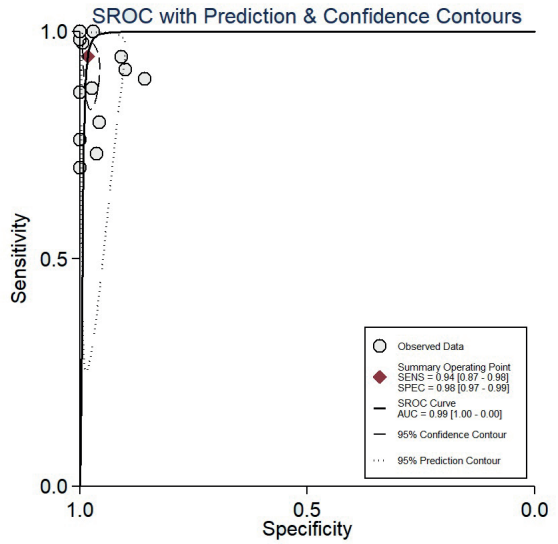

Figure 7. SROC Curve for MRI in the detection of bone metastasis.

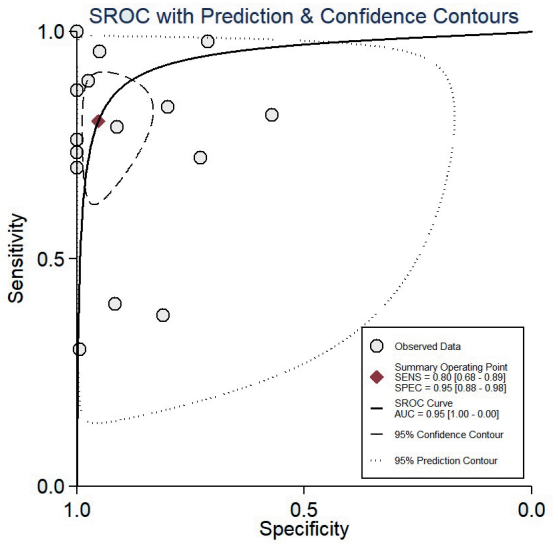

Figure 8. SROC Curve for SS in the detection of bone metastasis.

post-test probability for MRI (94% positive; 2% negative, Figure 9) and SS (84% positive, 6% negative, Figure 10) differed significantly from pre-test probability (23%).

Assessment of Heterogeneity and Publication Bias

There was substantial heterogeneity with the I^2 value of 99% and a chi-square test was significant ($p<0.001$). Bivariate box plot (Figure 11) shows that about 3 studies[16,32,34] were out of the circle indicating the heterogeneity between the included studies. Meta-regression results indicated that patient selection and flow, and timing of the test standard was the potential sources of heterogeneity in the model ($p<0.05$) (Figure 12). Finally, publication bias was tested through the funnel plot (Figure 13) and asymmetry of the plot was assessed using Deek's test. The symmetry of the funnel plot and the results of the Deek's test suggest no significant publication bias ($p=0.09$).

Discussion

To our knowledge, our meta-analysis is the first study that clearly shows that whole-body MRI is of greater sensitivity and higher, but comparable specificity when compared to skeletal scintigraphy. MRI has higher diagnostic accuracy and can be used for both confirmation and exclusion, while SS can be used for confirmation only.

Recent advances in the treatment of many cancers mean that there is an increase in the life expectancy of many patients with metastatic disease and a greater chance of developing skeletal metastases[37]. At present, no single imaging strategy is consistently superior for the early diagnosis and assessment of metastatic bone cancers[38].

While being widely used in diagnostics of bone metastases, skeletal scintigraphy's main limitation is its sensitivity and specificity. The sensitivity of 99Tc scintigraphy has been reported to range from 62 to 89%, with a false-positive rate as high as 40%[39]. SS relies on the osteoblastic response to skeletal destruction by tumor cells and the accompanying increase in regional blood flow[40].

Whole-body MRI is now feasible in scan times of less than 1 h, no need for contrast material, and can identify bone metastases early on, before the onset of host osteoblasts reaction[40]. While several studies addressed the differences in the efficiency of SS and MRI in the diagnosis of skeletal metastases, the results were inconclusive. In the last meta-analysis by Wu et al[13], that included 7 studies, both methods had a comparable diagnostic performance for detecting bone metastatic tumors. However, the analysis was unable to determine what method is superior in detecting bone metastases. In our meta-analysis, we used summary estimates and SROC curves to assess the diagnostic accuracy of whole-body MRI and skeletal scintigraphy from 15 studies[14,16,17,21,26-36].

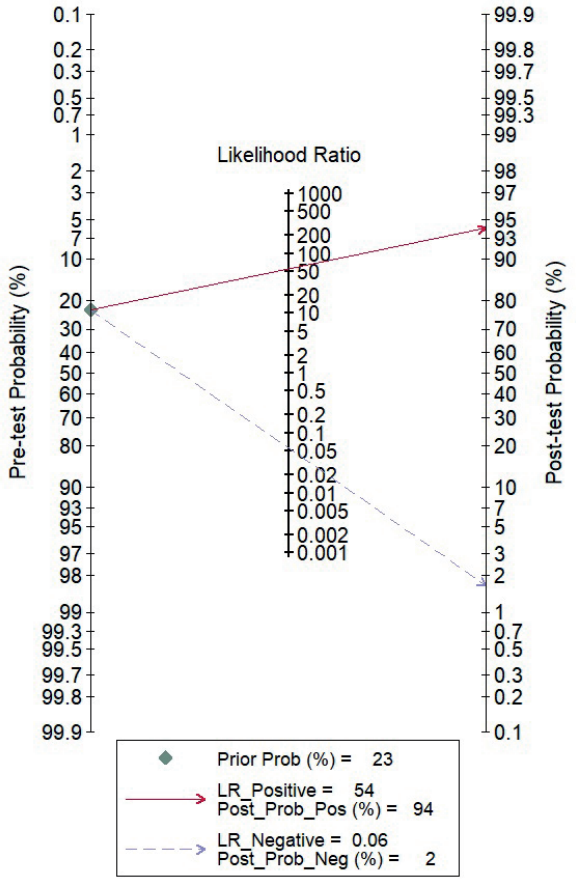

Figure 9. Fagan nomogram evaluating the overall value of MRI for the diagnosis of bone metastasis.

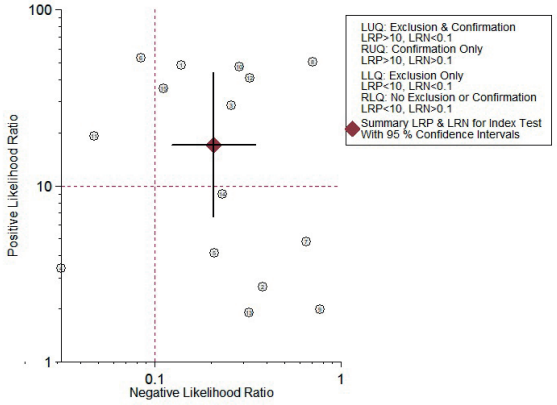

Figure 10. Fagan nomogram evaluating the overall value of SS for the diagnosis of bone metastasis.

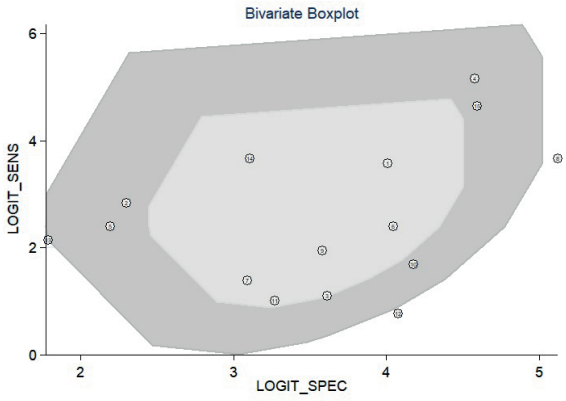

Figure 11. Bivariate boxplot of the sensitivity and specificity in the included studies.

Whole-body MRI showed higher sensitivity than SS (an increase of 14%), and slightly higher, but comparable specificity (99% *vs.* 95%) in detecting bone metastases.

The AUC is an index of the overall performance of a test with values ranging between 1 and 0, where 1 indicates a perfect test that correctly distinguishes between cases of disease and non-cases of disease, and value of 0 indicates a test that fails to diagnose[41]. In our study, both SS and MRI had comparably high AUC values (0.99 and 0.95 respectively), indicating that these two methods are highly effective in diagnostics on skeletal metastases.

Fagan's nanogram is a tool to determine diagnostic test characteristics (sensitivity, specificity, likelihood ratios) and/or determine the post-test probability of disease given the pre-test probability and test characteristics[42]. In our study, for both methods pre-test probability (23%) differed significantly from the post-test one (94% positive; 2% negative for MRI, and 84% positive, 6% negative for SS).

Diagnostic odds ratio (DOR) was used to investigate multiple relationships between the chances of obtaining positive and negative results. DOR is a comprehensive evaluation index in diagnostic tests, as it shows the ratio of the odds of a positive test in a patient with disease relative to the odds of the positive test in a patient that does not have a disease[41,43]. A good diagnostic test should have DOR>100, with LPR above 10 and LNR<0.1[41]. We demonstrated that MRI performs better as a diagnostic imaging method, with DOR of 966, as compared to DOR of 82 for SS. We used LPR and LNR as measures of diagnostic accuracy, as higher LPR in combination with lower LNR. Our analysis shows that whole-body MRI has 3.18-fold higher LPR than SS (54.4 *vs.* 17.1 respectively) in combination with an LNR value of 0.06, which is below 0.1. This positions a summary LPR and LNR in the upper left quadrant of the likelihood scattergram, indicating that MRI can be used for

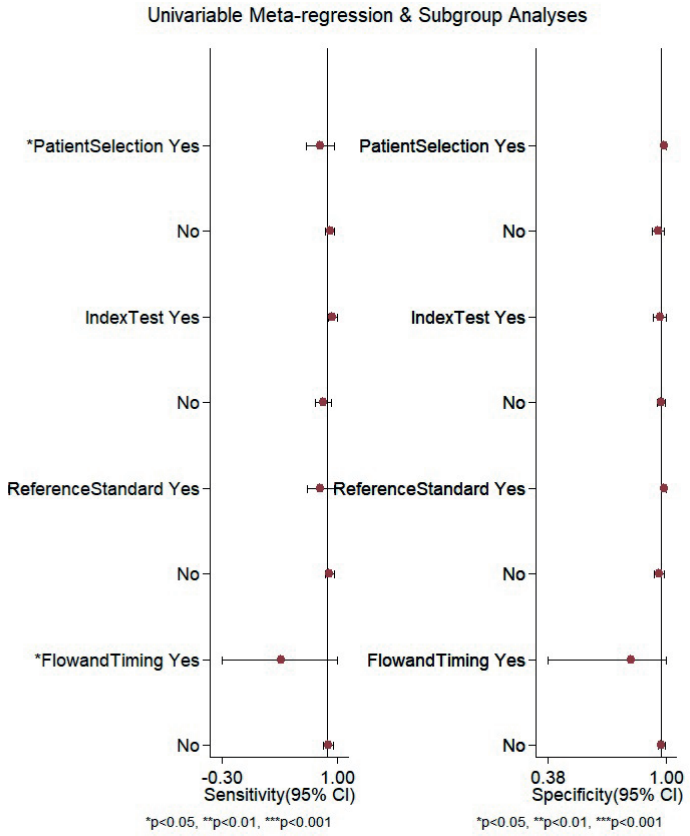

Figure 12. Meta regression for sources of heterogeneity among the studies included.

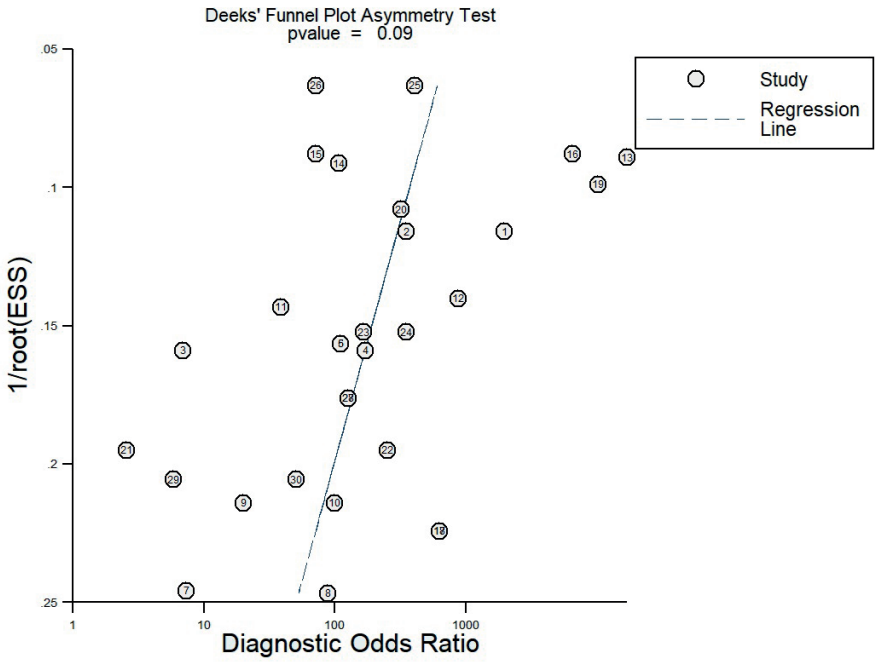

Figure 13. Funnel plot for publication bias.

both confirmation and exclusion of bone metastases. At the same time, while the LPR value of SS was still above 10 (17.1), the LNR value of SS was 0.22, which is above 0.1. The likelihood scattergram clearly showed that SS can be used for confirmation only. Taken together, DOR, LNR and LPR values show that whole-body MRI has a better discriminating ability than SS. Moreover, as indicated by the LNR value of MRI, our analysis suggests that this method can be used alone to rule out bone metastases.

Our meta-analysis has some limitations. There was substantial heterogeneity between the included studies. It is well established that differences in study design and patient selection have a substantial impact on estimates of diagnostic accuracy. In studies, where patients were selected on the basis of whether they had been referred for the index test rather than on clinical symptoms, the diagnostic accuracy may be lower, while in retrospective studies, and in studies with nonconsecutive inclusion of patients, the accuracy may be higher[44].

Conclusions

In summary, we showed for the first time a clear advantage of using whole-body MRI for the diagnosis of bone metastases. It has higher sensitivity than skeletal scintigraphy, as well as higher diagnostic accuracy, and can be used for both confirmation and exclusion of metastatic bone disease.

Authors' contributions

GS and YZ designed the meta-analysis; FL and NT searched the literature; GS, YZ and FL analyzed the literature; GS and YZ wrote the manuscript; NT edited the manuscript.

Conflict of Interest

The Authors declare that they have no conflict of interests.

References

1) Vassiliou V, Andreopoulos D, Frangos S, Tselis N, Giannopoulou E, Lutz S. Bone metastases: assessment of therapeutic response through radiological and nuclear medicine imaging modalities. Clin Oncol (R Coll Radiol) 2011; 23: 632-645.
2) Ibrahim T, Flamini E, Fabbri L, Serra P, Mercatali L, Ricci R, Sacanna E, Falasconi MC, Casadei R, Galassi R, Giannini M, Bazzocchi O, Calzolari F, Nunziatini R, Gaudio M, Maltoni M, Amadori D. Multidisciplinary approach to the treatment of bone metastases: Osteo-Oncology Center, a new organizational model. T Tumori 2009; 95: 291-297.
3) Plunkett TA, Rubens RD. The biology and management of bone metastases. Crit Rev Oncol Hematol 1999; 31: 89-96.
4) Mundy GR. Metastasis to bone: causes, consequences and therapeutic opportunities. Nat Rev Cancer 2002; 2: 584-593.
5) O'Sullivan GJ, Carty FL, Cronin CG. Imaging of bone metastasis: an update. World J Radiol 2015; 7: 202-211.
6) Shie P, Cardarelli R, Brandon D, Erdman W, Abdulrahim N. Meta-analysis: comparison of F-18 Fluorodeoxyglucose-positron emission tomography and bone scintigraphy in the detection of bone metastases in patients with breast cancer. Clin Nucl Med 2008; 33: 97-101.
7) Abe K, Sasaki M, Kuwabara Y, Koga H, Baba S, Hayashi K, Takahashi N, Honda H. Comparison of 18FDG-PET with 99mTc-HMDP scintigraphy for the detection of bone metastases in patients with breast cancer. Ann Nucl Med 2005; 19: 573-579.
8) Rong J, Wang S, Ding Q, Yun M, Zheng Z, Ye S. Comparison of 18 FDG PET-CT and bone scintigraphy for detection of bone metastases in breast cancer patients. A meta-analysis. Surg Oncol 2013; 22: 86-91.
9) Koizumi M, Matsumoto S, Takahashi S, Yamashita T, Ogata E. Bone metabolic markers in the evaluation of bone scan flare phenomenon in bone metastases of breast cancer. Clin Nucl Med 1999; 24: 15-20.
10) Costelloe CM, Rohren EM, Madewell JE, Hamaoka T, Theriault RL, Yu TK, Lewis VO, Ma J, Stafford RJ, Tari AM, Hortobagyi GN, Ueno NT. Imaging bone metastases in breast cancer: techniques and recommendations for diagnosis. Lancet Oncol 2009; 10: 606-614.
11) Yang HL, Liu T, Wang XM, Xu Y, Deng SM. Diagnosis of bone metastases: a meta-analysis comparing ^{18}FDG PET, CT, MRI and bone scintigraphy. Eur Radiol 2011; 21: 2604-2617.
12) Wu LM, Gu HY, Zheng J, Xu X, Lin LH, Deng X, Zhang W, Xu JR. Diagnostic value of whole-body magnetic resonance imaging for bone metastases: a systematic review and meta-analysis. J Magn Reson Imaging 2011; 34: 128-135.
13) Ohlmann-Knafo S, Kirschbaum M, Fenzl G, Pickuth D. Diagnostic value of whole-body MRI and bone scintigraphy in the detection of osseous metastases in patients with breast cancer--A Prospective Double-Blinded Study at two Hospital Centers. Rofo 2009; 181: 255-263.
14) Ketelsen D, Röthke M, Aschoff P, Merseburger AS, Lichy MP, Reimold M, Claussen CD, Schlemmer HP. Detection of bone metastasis of prostate cancer - comparison of whole-body MRI and bone scintigraphy. Rofo 2008; 180: 746-752.
15) Lecouvet FE, El Mouedden J, Collette L, Coche E, Danse E, Jamar F, Machiels JP, Vande Berg B, Omoumi

P, Tombal B. Can whole-body magnetic resonance imaging with diffusion-weighted imaging replace Tc 99m bone scanning and computed tomography for single-step detection of metastases in patients with high-risk prostate cancer? Eur Urol 2012; 62: 68-75.

16) Sohaib SA, Cook G, Allen SD, Hughes M, Eisen T, Gore M. Comparison of whole-body MRI and bone scintigraphy in the detection of bone metastases in renal cancer. Br J Radiol 2009; 82: 632-639.

17) Eustace S, Tello R, DeCarvalho V, Carey J, Wroblicka JT, Melhem ER, Yucel EK. A comparison of whole-body turboSTIR MR imaging and planar 99mTc-methylene diphosphonate scintigraphy in the examination of patients with suspected skeletal metastases. AJR Am J Roentgenol 1997; 169: 1655-1661.

18) Steinborn MM, Heuck AF, Tiling R, Bruegel M, Gauger L, Reiser MF. Whole-body bone marrow MRI in patients with metastatic disease to the skeletal system. J Comput Assist Tomogr 1999; 23: 123-129.

19) Lauenstein TC, Freudenberg LS, Goehde SC, Ruehm SG, Goyen M, Bosk S, Debatin JF, Barkhausen J. Whole-body MRI using a rolling table platform for the detection of bone metastases. Eur Radiol 2002; 12: 2091-2099.

20) Engelhard K, Hollenbach HP, Wohlfart K, von Imhoff E, Fellner FA. Comparison of whole-body MRI with automatic moving table technique and bone scintigraphy for screening for bone metastases in patients with breast cancer. Eur Radiol 2004; 14: 99-105.

21) Ghanem N, Altehoefer C, Kelly T, Lohrmann C, Winterer J, Schäfer O, Bley TA, Moser E, Langer M. Whole-body MRI in comparison to skeletal scintigraphy in detection of skeletal metastases in patients with solid tumors. In Vivo 2006; 20: 173-182.

22) Frat A, AÐildere M, GençoÐlu A, Cakir B, Akin O, Akcali Z, Aktaş A. Value of whole-body turbo short tau inversion recovery magnetic resonance imaging with panoramic table for detecting bone metastases: comparison with 99MTc-methylene diphosphonate scintigraphy. J Comput Assist Tomogr 2006; 30: 151-156.

23) Ben-Haim S, Israel O. Breast cancer: role of SPECT and PET in imaging bone metastases. Semin Nucl Med 2009; 39: 408-415.

24) Beheshti M, Langsteger W, Fogelman I. Prostate cancer: role of SPECT and PET in imaging bone metastases. Semin Nucl Med 2009; 39: 396-407.

25) Daldrup-Link HE, Franzius C, Link TM, Laukamp D, Sciuk J, Jürgens H, Schober O, Rummeny EJ. Whole-body MR imaging for detection of bone metastases in children and young adults: comparison with skeletal scintigraphy and FDG PET. AJR Am J Roentgenol 2001; 177: 229-236.

26) Takenaka D, Ohno Y, Matsumoto K, Aoyama N, Onishi Y, Koyama H, Nogami M, Yoshikawa T, Matsumoto S, Sugimura K. Detection of bone metastases in non-small cell lung cancer patients: comparison of whole-body diffusion-weighted imaging (DWI), whole-body MR imaging without and with DWI, whole-body FDG-PET/CT, and bone scintigraphy. J Magn Reson Imaging 2009; 30: 298-308.

27) Venkitaraman R, Cook GJ, Dearnaley DP, Parker CC, Khoo V, Eeles R, Huddart RA, Horwich A, Sohaib SA. Whole-body magnetic resonance imaging in the detection of skeletal metastases in patients with prostate cancer. J Med Imaging Radiat Oncol 2009; 53: 241-247.

28) Balliu E, Boada M, Peláez I, Vilanova JC, Barceló-Vidal C, Rubio A, Galofré P, Castro A, Pedraza S. Comparative study of whole-body MRI and bone scintigraphy for the detection of bone metastases. Clin Radiol 2010; 65: 989-996.

29) Kim DS, Hong SH, Choi JY, Paeng JC, Kim NR, Jun WS, Kang HS. Magnetic resonance imaging diagnoses of bone scan abnormalities in breast cancer patients. Nucl Med Commun 2009; 30: 736-741.

30) Earnest F 4th, Ryu JH, Miller GM, Luetmer PH, Forstrom LA, Burnett OL, Rowland CM, Swensen SJ, Midthun DE. Suspected non-small cell lung cancer: incidence of occult brain and skeletal metastases and effectiveness of imaging for detection-pilot study. Radiology 1999; 211: 137-145.

31) Layer G, Steudel A, Schüller H, van Kaick G, Grünwald F, Reiser M, Schild HH. Magnetic resonance imaging to detect bone marrow metastases in the initial staging of small cell lung carcinoma and breast carcinoma. Cancer 1999; 85: 1004-1009.

32) Xu X, Ma L, Zhang JS, Cai YQ, Xu BX, Chen LQ, Sun F, Guo XG. Feasibility of whole body diffusion weighted imaging in detecting bone metastasis on 3.0T MR scanner. Chin Med Sci J 2008; 23: 151-157.

33) Kumar J, Seith A, Kumar A, Sharma R, Bakhshi S, Kumar R, Agarwala S. Whole-body MR imaging with the use of parallel imaging for detection of skeletal metastases in pediatric patients with small-cell neoplasms: comparison with skeletal scintigraphy and FDG PET/CT. Pediatr Radiol 2008; 38: 953-962.

34) Altehoefer C, Ghanem N, Högerle S, Moser E, Langer M. Comparative detectability of bone metastases and impact on therapy of magnetic resonance imaging and bone scintigraphy in patients with breast cancer. Eur J Radiol 2001; 40: 16-23.

35) Jambor I, Kuisma A, Ramadan S, Huovinen R, Sandell M, Kajander S, Kemppainen J, Kauppila E, Auren J, Merisaari H, Saunavaara J, Noponen T, Minn H, Aronen HJ, Seppänen M. Prospective evaluation of planar bone scintigraphy, SPECT, SPECT/CT, 18F-NaF PET/CT and whole body 1.5T MRI, including DWI, for the detection of bone metastases in high risk breast and prostate cancer patients: SKELETA clinical trial. Acta Oncol 2016; 55: 59-67.

36) Gralow JR, Biermann JS, Farooki A, Fornier MN, Gagel RF, Kumar R, Litsas G, McKay R, Podoloff DA, Srinivas S, Van Poznak CH. NCCN Task Force Report: Bone Health In Cancer Care. J Natl Compr Canc Netw 2013; 11 Suppl 3: S1-50; quiz S51.

37) Roberts CC, Daffner RH, Weissman BN, Bancroft L, Bennett DL, Blebea JS, Bruno MA, Fries IB, Germano

IM, Holly L, Jacobson JA, Luchs JS, Morrison WB, Olson JJ, Payne WK, Resnik CS, Schweitzer ME, Seeger LL, Taljanovic M, Wise JN, Lutz ST. ACR appropriateness criteria on metastatic bone disease. J Am Coll Radiol 2010; 7: 400-409.

38) Cook GJR, Azad GK, Goh V. Imaging bone metastases in breast cancer: staging and response assessment. J Nucl Med 2016; 57 Suppl 1: 27S-33S.

39) Heindel W, Gübitz R, Vieth V, Weckesser M, Schober O, and Schäfers M. The diagnostic imaging of bone metastases. Dtsch Arztebl Int 2014; 111: 741-747.

40) Walter SD. Properties of the summary receiver operating characteristic (SROC) curve for diagnostic test data. Stat Med 2002; 21: 1237-1256.

41) Fagan TJ, Letter: Nomogram for Bayes theorem. N Engl J Med 1975; 293: 257.

42) Jones CM, Athanasiou T, Summary receiver operating characteristic curve analysis techniques in the evaluation of diagnostic tests. Ann Thorac Surg 2005; 79: 16-20

43) Rutjes, AW, Reitsma JB, Di Nisio M, Smidt N, van Rijn JC, Bossuyt PM. Evidence of bias and variation in diagnostic accuracy studies. CMAJ 2006; 174: 469-476.